[논 문] 한국재료학회지
Korean J. Mater. Res.
Vol. 33, No. 5 (2023)
https://doi.org/10.3740/MRSK.2023.33.5.189

First-Principles Investigation on the Electromechanical Properties of Monolayer 1H Pb-Dichalcogenides

Nguyen Hoang Linh[1], Nguyen Minh Son[1], Tran The Quang[2], Nguyen Van Hoi[3], Vuong Thanh[1], and Do Van Truong[1,4†]

[1]School of Mechanical Engineering, Hanoi University of Science and Technology, Hanoi 100000, Vietnam
[2]Department of Basic Engineering, Faculty of Technology, Thai Binh University, Thaibinh 410000, Vietnam
[3]Department of Mechanical System Engineering, Jeonbuk National University, Jeonju 54896, Republic of Korea
[4]International Research Center for Computational Materials Science, Hanoi University of Science and Technology, Hanoi 100000, Vietnam

(Received August 3, 2022 : Revised March 8, 2023 : Accepted April 4, 2023)

Abstract This study uses first-principles calculations to investigate the mechanical properties and effect of strain on the electronic properties of the 2D material 1H-PbX_2 (X: S, Se). Firstly, the stability of the 1H Pb-dichalcogenide structures was evaluated using Born's criteria. The obtained results show that the 1H-PbS_2 material possesses the greatest ideal strength of 3.48 N/m, with 3.68 N/m for 1H-$PbSe_2$ in biaxial strain. In addition, 1H-PbS_2 and 1H-$PbSe_2$ are direct semiconductors at equilibrium with band gaps of 2.30 eV and 1.90 eV, respectively. The band gap was investigated and remained almost unchanged under the strain ε_{xx} but altered significantly at strains ε_{yy} and ε_{bia}. At the fracture strain in the biaxial direction (19 %), the band gap of 1H-PbS_2 decreases about 60 %, and that of 1H-$PbSe_2$ decreases about 50 %. 1H-PbS_2 and 1H-$PbSe_2$ can convert from direct to indirect semiconductor under the strain ε_{yy}. Our findings reveal that the two structures have significant potential for application in nanoelectronic devices.

Key words 2D material, band gap, semiconductor materials, mechanical properties, ideal strength.

1. Introduction

Low-dimensional (2D) materials such as graphene,[1)] boron nitride[2)] have been attracting special attention of scientists due to their unusual mechanical and electronic properties. Following those findings, other groups of 2D materials such as chalcogenides,[3,4)] dichalcogenides,[5,6)] borophene[7)] have been discovered and studied. Their distinct electronic and thermal properties are also revealed in turning and becoming important bases for applications in micro-electromechanical systems, opto-electrical devices, thermoelectrics, sensors.[2,5,6,8,9)]

The group of chalcogenide materials containing lead (Pb) exists in numerous distinct structures, comprising α, β, γ, 1T and 1H,[10-12)] that have been proven to have high potential for applications in electronic and optical devices. Previous studies have primarily focused on the α, β, γ or 1T structures, while the 1H-PbX_2 structure has not been widely investigated. Jin et al. have indicated that the multifunctional material structure PbS_2 has a negative Poisson's ratio and electronic properties that can be controlled by strain.[13)] In the study by Quain, the heterostructure of Pb coated on WS_2 material has the potential to enhance the performance of the devices, facilitating the development of optoelectronic applications.[10)] The electronic and thermal properties of several chalcogenide materials containing Pb have also been explored.[14)] Meanwhile, 1H-MX_2 structures with M of transition metal, that have many practical applications, such as high-efficiency electroreduction,[15)]

†Corresponding author
E-Mail : truong.dovan@hust.edu.vn (D. V. Truong, Hanoi Univ. Sci. Technol.)

conversion and generation of new energy sources, and other applications.[16] Therefore, in this paper, we investigate the mechanical and electronic properties of 1H-PbS_2 and 1H-$PbSe_2$ in order to determine their potential applications in the near future.

2. Simulation

In this study, all calculations were performed by the density functional theory (DFT)[17,18] with Perdew-Burke-Ernzeholf exchange correlation potential energy (PBE) using the generalized gradient approximation (GGA)[19] implemented in Quantum Espresso package.[20] The kinetic energy cutoff was chosen as 60 Ry for the wave function and 700 Ry for the charge density. The kpoint grid in the Birilluoin region was selected as 15 × 15 × 1 according to the Monkhorst-Pack method.[21] Fig. 1 depicts the atomic structures of 1H-PbS_2 and 1H-$PbSe_2$. Periodic boundary conditions were applied on all three x, y, z directions of the model. The vacuum region in the z direction was set to 30Å to avoid interaction between atomic layers. The equilibrium structure was obtained by the Broyden-Fletcher-Goldfarb-Shanno (BFGS) minimum energy method with the stress components less than 5.10^{-2} GPa and the force conditions less than 5.10^{-6} Ry/a.u at the temperature 0K.[22] The elastic constants are calculated using the Thermo-Pw algorithm.[23] The structure is investigated under the strain

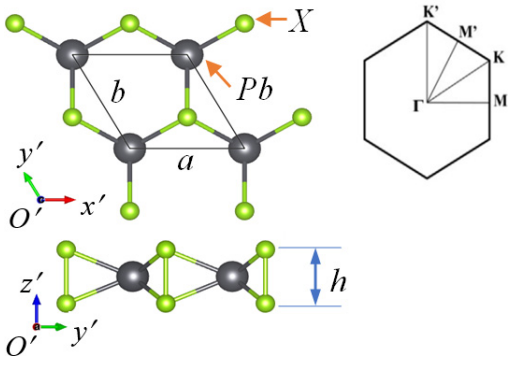

Fig. 1. Atomic model of 1H-PbX_2 (X: S, Se) and the region of Brillouin.

in the x, y and biaxial directions with the step of 1 % until the material structure is fracture. The strain is defined by $\varepsilon = (a - a_0) / a_0$, where a and a_0 are lattice constants of 1H-PbX_2 (X: S, Se) after and before applying the strain.

Eqs. (1) and (2) are given to determine the elastic moduli E_{xx}, E_{yy} and Poisson's ratios υ_{xy}, υ_{yx} via the elastic constants C_{ij}:[6,24]

$$E_{xx} = \frac{C_{11}C_{22} - C_{12}^2}{C_{11}};\ E_{yy} = \frac{C_{22}C_{11} - C_{12}^2}{C_{22}} \quad (1)$$

$$\upsilon_{xy} = \frac{C_{11}}{C_{12}};\ \upsilon_{yx} = \frac{C_{22}}{C_{12}} \quad (2)$$

3. Result and Discussion

Based on the density functional theory, the material parameters such as lattice constant a, b, elastic constant C_{ij} determined are listed in Table 1. The obtained results show that the lattice constant increases as the element X changing from S to Se as a = b = 4.73 (Å) and a = b = 4.88 (Å), respectively. The gradual increase of the lattice constant is due to the increasing radius of chalcogenide elements.

Based on Born's criterion[25] with $C_{11} > |C_{12}| > 0$ and $C_{66} > 0$, two material structures confimed to be stable. The elastic modulus of monolayer structures 1H-PbS_2 and 1H-$PbSe_2$ are $E_{xx} = E_{yy} = 3.54$ N/m and $E_{xx} = E_{yy} = 2.48$ N/m, respectively, which are significantly smaller than the elastic modulus of other 2D structures such as $GaInTe_3$ (113 N/m)[26] or Janus WSSe (137.7 N/m)[27] or 1H-WS_2 (220 N/m).[6] This result shows that the monolayer structures 1H-PbS_2 and 1H-$PbSe_2$ can be used in applications with large mechanical strain.

Fig. 2 shows the stress-strain relationship in the x, y and biaxial directions. Due to the monolayer structure, the stress is calculated as the product of the unit cell stress (N/m^2) and the unit cell thickness (30 Å).[28] Generally, the stress-strain relationship of the two structures is similar in all three direc-

Table 1. Lattice constant a and b (Å), thickness h (Å), elastic constant C_{ij} (N/m), elastic modulus E (N/m) and Poisson's ratio υ of 1H-PbS_2, 1H-$PbSe_2$ materials.

Material	a = b	h	C_{11}	C_{22}	C_{12}	C_{66}	$E_{xx} = E_{yy}$	$\upsilon_{xy} = \upsilon_{yx}$
1H-PbS_2	4.73	2.15	28.70	28.70	26.87	0.86	3.54	0.94
1H-$PbSe_2$	4.88	2.42	25.90	25.90	24.63	0.64	2.48	0.95

tions x, y and biaxial. The ideal strain of 1H-PbS_2 is higher than that of 1H-$PbSe_2$ in all three directions. The maximum stress in the x direction of 1H-PbS_2 [Fig. 2(a)] is 0.15 N/m at ε_{xx} = 7 %, about 0.04 N/m higher than 1H-$PbSe_2$. Under the strain ε_{yy}, two materials are failed at the relatively large strain (ε_{yy} = 22 %) with the critical stress of 1.03 N/m for 1H-PbS_2 and 0.88 N/m for 1H-$PbSe_2$. Finally, the critical stresses in the biaxial direction of 1H-PbS_2 and 1H-$PbSe_2$ are 3.48 N/m and 3.68 N/m, respectively at the strain of 19 %. The strength of 1H-PbS_2 is higher than that of 1H-$PbSe_2$ because the electronegativity of S (χ = 2.58) is greater than that of Se (χ = 2.55), which makes the bond of Pb-S more difficult to break than that of Pb-Se.

To understand more the strain effect on the electronic properties, the band structure of 1H-PbS_2 and 1H-$PbSe_2$ is investigated at several strains. In Figs. 3 and 4, 1H-PbS_2 and 1H-$PbSe_2$ possess the band gap at the equilibrium (ε = 0 %) of 2.30 eV and 1.90 eV, respectively. The results show that two materials are both the direct semiconductors with the conduction-band minimum and the valence-band maximum both at the point. Fig. 3 shows the strain effect in the x and y directions on the band gap of 1H-PbS_2. Under the strain ε_{xx},

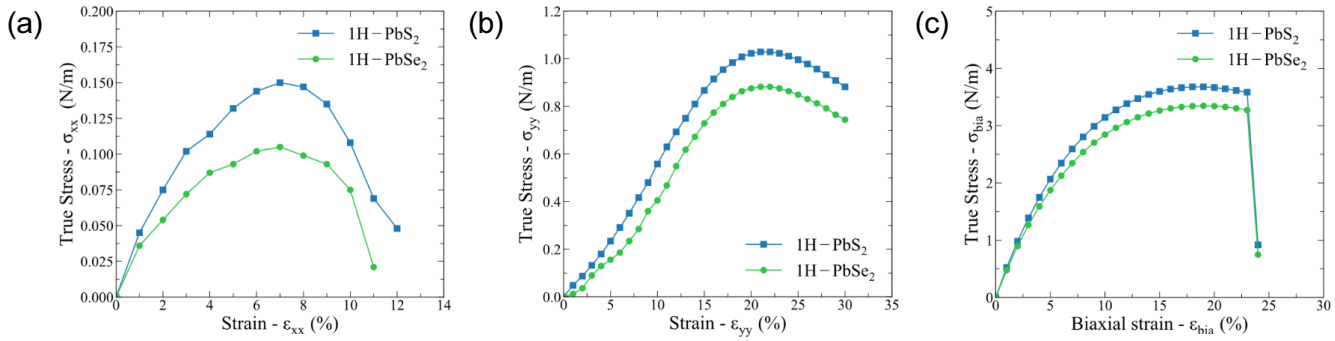

Fig. 2. Stress-strain relationship of structures 1H-PbS_2 and 1H-$PbSe_2$: (a) in the x direction; (b) in the y direction and (c) in the biaxial direction.

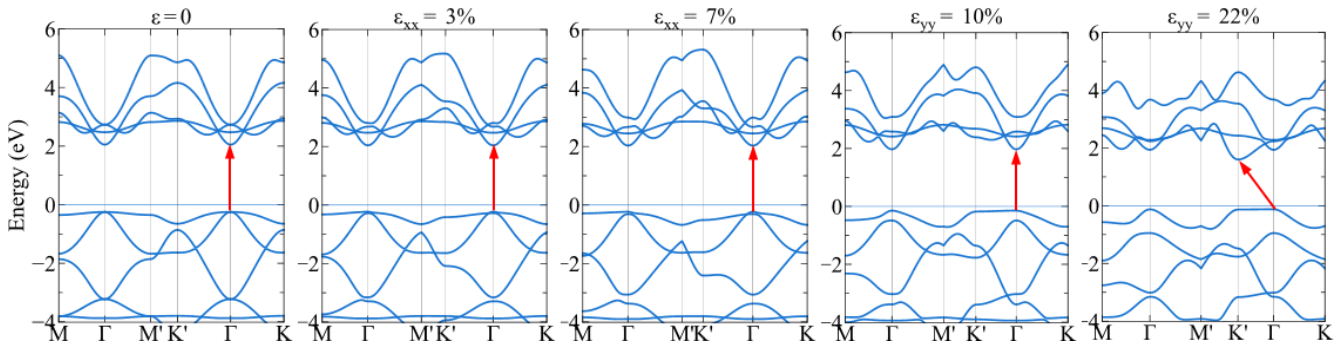

Fig. 3. Band structure of 1H-PbS_2 at several strains in the x and y directions.

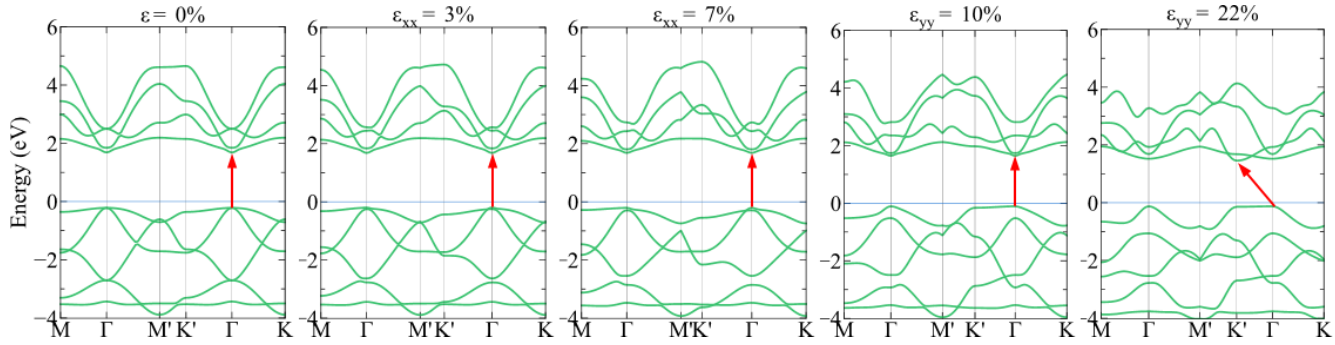

Fig. 4. Band structure of 1H-$PbSe_2$ at several strains in the x and y directions.

the band gap insignificant change at the fracture strain (ε_{xx} = 7 %). The material remains the direct semiconductor. Under the strain ε_{yy}, the band gap tends to decrease. The valence-band maximum remains at the Γ point, however the conduction-band minimum moves from the point to K'. The material changes from the direct semiconductor to the indirect semiconductor in this case.

Fig. 4 shows the energy band structure of 1H-$PbSe_2$ at several strains in the x and y directions. Similar to 1H-PbS_2, the obtained results show that 1H-$PbSe_2$ remains the direct semiconductor, and the band gap does not change significantly under the tensile strain ε_{xx}. The material also changes from the direct semiconductor to the indirect semiconductor under the strain ε_{yy} = 22 %.

In Fig. 5, under the strain ε_{bia}, 1H-PbS_2 and 1H-$PbSe_2$ both exhibit the direct semiconductor, however their band gap decreases significantly with increasing the strain. At the equilibrium (0 %), 1H-PbS_2 and 1H-$PbSe_2$ possess the band gap of 2.3 eV and 1.9 eV respectively, but at the fracture strain (19 %), the band gap of 1H-PbS_2 is decreased about 60 % and 1H-$PbSe_2$ decreased about 50 %.

The relationship between the band gap and strain is shown in Fig. 6. Overall, results express that the band gap in almost constant under the stain ε_{xx}, Fig. 6(a). Under the strain ε_{yy}, the band gap of 1H-PbS_2 declines slightly. While, the band gap of 1H-$PbSe_2$ decreases more significant than of 1H-PbS_2. The least band gap of both models is 1.71 eV (decreasing by 25.5 %), 1.6 eV (decreasing by 16 %) respectively relating ε_{yy} =

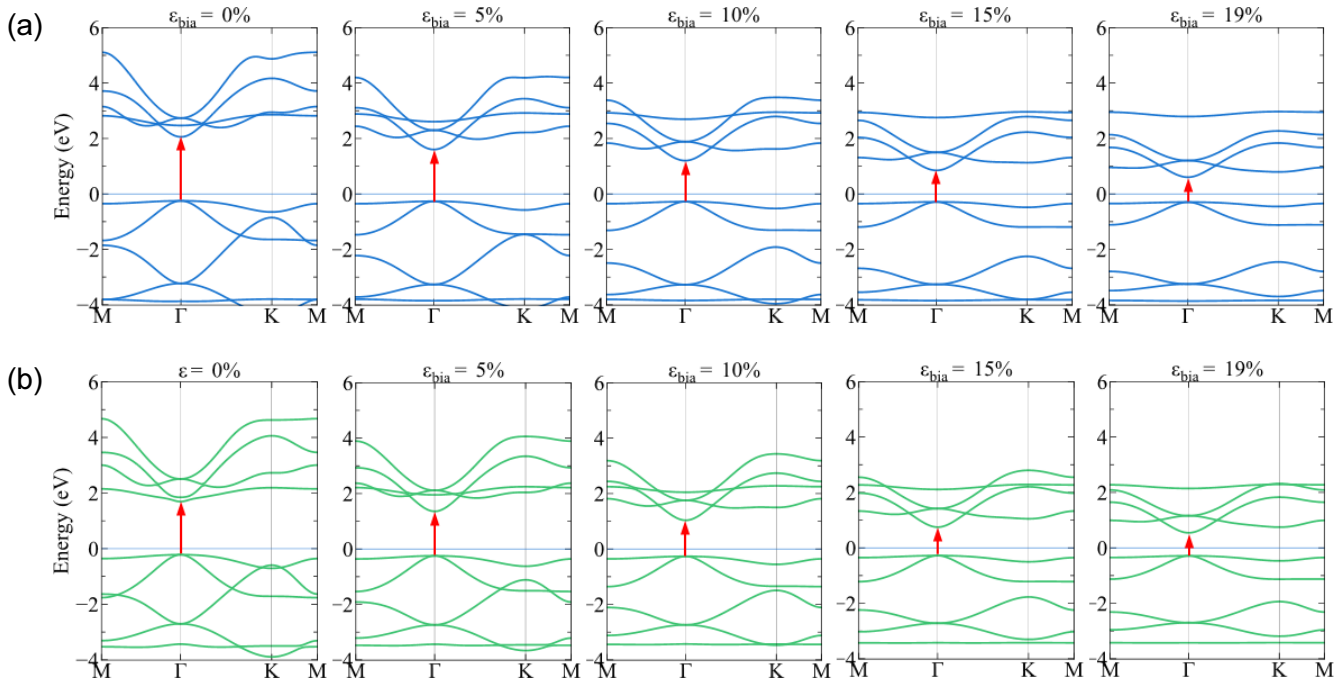

Fig. 5. Band structures at several strain ε_{bia} of: (a) 1H-PbS_2 (b) 1H-$PbSe_2$.

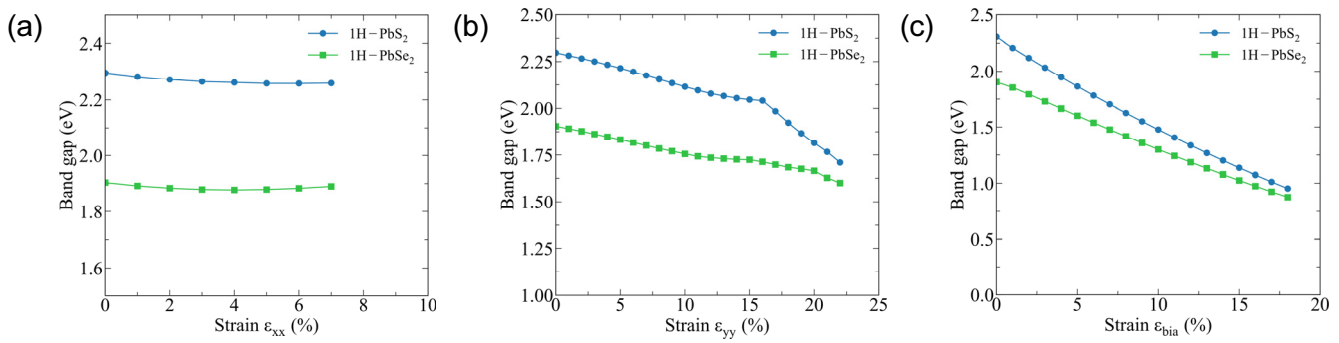

Fig. 6. Strain-band gap relationship of 1H-PbS_2 and 1H-$PbSe_2$: (a) in the x direction, (b) in the y direction and (c) in the biaxial direction.

22 %, Fig. 6(b). Additionally, under biaxial strain, the band gap of 1H-PbS_2 and 1H-$PbSe_2$ plummetes swiftly to destructive strain (ε_{bia} = 19 %), as illustration above. To sum up, the band gap is function of mechanical deformation. Each strains and kind of deformation will have sole band gap. While, the band gap involving strain ε_{xx} has moderately change, the band gap of strain ε_{yy} and ε_{bia} decline dramatically to fracture strain in both structures 1H-PbS_2 and 1H-$PbSe_2$. Moreover, the obtained results show that the 1H-PbS_2 and 1H-$PbSe_2$ account the particularly band gap, direct and indirect properties that can be changed through mechanical deformation under the strains ε_{xx}, ε_{yy} and ε_{bia}. This change is similar to the Janus TMDs MoSSe, WSTe, WSeTe.[27] The obtained results once again confirm that the band gap of the material can be controlled by mechanical strain.

4. Conclusions

Based on the density function theory, the mechanical properties and the strain effect on the electronic properties of 2D material 1H-PbX_2 (X: S, Se) are investigated. The obtained results show that the materials possess the greatest ideal strength in the biaxial strain with 1H-PbS_2 of 3.48 N/m and 1H-$PbSe_2$ of 3.68 N/m. At the equilibrium (0 %), 1H-PbS_2 and 1H-$PbSe_2$ are both the direct semiconductors with their band gaps of 2.30 eV and 1.90 eV, respectively. Under the strain ε_{xx}, the band gap of two materials is almost unchanged, however they alter significantly under the strains ε_{yy} and ε_{bia}. At the fracture strain in the biaxial direction (19 %), the band gap of 1H-PbS_2 decreased about 60 % and that of 1H-$PbSe_2$ decreased about 50 %. Interestingly, under the strain ε_{yy}, 1H-PbS_2 and 1H-$PbSe_2$ convert from the direct to the indirect semiconductor. The results obtained above are an important basis for using mechanical strain to control the band gap as well as to convert materials from the direct to the indirect semiconductor.

References

1. M. Devi and A. Kumar, Mater. Res. Bull., **97**, 207 (2018).
2. K. S. Novoselov, V. I. Fal'ko, L. Colombo, P. R. Gellert, M. G. Schwab and K. Kim, Nature, **490**, 192 (2012).
3. A. L. Elías, N. Perea-López, A. Castro-Beltrán, A. Berkdemir, R. Lv, S. Feng, A. D. Long, T. Hayashi, Y. A. Kim, M. Endo, H. R. Gutiérrez, N. R. Pradhan, L. Balicas, T. E. Mallouk, F. López-Urías, H. Terrones and M. Terrones, ACS Nano, **7**, 5235 (2013).
4. B. Ge, B. Chen and L. Li, Appl. Surf. Sci., **550**, 149177 (2021).
5. M. S. Sokolikova and C. Mattevi, Chem. Soc. Rev., **49**, 3952 (2020).
6. V. Van Thanh, N. T. Hung and D. Van Truong, RSC Adv., **8**, 38667 (2018).
7. M. Isa Khan, A. Majid, N. Ashraf and I. Ullah, Phys. Chem. Chem. Phys., **22**, 3304 (2020).
8. E. Gourmelon, O. Lignier, H. Hadouda, G. Couturier, J. C. Bernde, J. Tedd, J. Pouzet and J. Salardenne, Sol. Energy Mater. Sol. Cells, **46**, 115 (1997).
9. V. K. Sangwan and M. C. Hersam, Annu. Rev. Phys. Chem., **69**, 299 (2018).
10. M. Y. Qian, Z. L. Yu, Q. Wan, P. B. He, B. Liu, J. L. Yang, C. M. Xu and M. Q. Cai, Phys. Status Solidi RRL, **14**, 2000016 (2020).
11. T. Kocabas, D. Cakir and C. Sevik, J. Phys.: Condens. Matter, **33**, 115705 (2021).
12. B. Ul Haq, S. AlFaify, R. Ahmed, A. Laref, Q. Mahmood and E. Algrafy, Appl. Surf. Sci., **525**, 146521 (2020).
13. W. Jin, J. Pang, L. Yue, M. Xie, X. Kuang and C. Lu, J. Phys. Chem. Lett., **13**, 10494 (2022).
14. Y. I. Ravich, B. A. Efimova and I. A. Smirnov, Semiconducting Lead Chalcogenides, 1st ed., p.149, Springer, New York (1970).
15. J. Xu, S. Lai, M. Hu, S. Ge, R. Xie, F. Li, D. Hua, H. Xu, H. Zhou, R. Wu, J. Fu, Y. Qiu, J. He, C. Li, H. Liu, Y. Liu, J. Sun, X. Liu and J. Luo, Small Methods, **4**, 2000567 (2020).
16. N. Choudhary, M. A. Islam, J. H. Kim, T.-J. Ko, A. Schropp, L. Hurtado, D. Weitzman, L. Zhai and Y. Jung, Nano Today, **19**, 16 (2018).
17. M. Morales, R. Clay, C. Pierleoni and D. Ceperley, Entropy, **16**, 287 (2013).
18. G. Kresse and J. Furthmüller, Phys. Rev. B, **54**, 11169 (1996).
19. P. P. John, B. Kieron and E. Matthias, Phys. Rev. Lett., **77**, 3865 (1996).
20. P. Giannozzi, S. Baroni, N. Bonini, M. Calandra, R. Car, C. Cavazzoni, D. Ceresoli, G. L. Chiarotti, M. Cococcioni, I. Dabo, A. Dal Corso, S. de Gironcoli, S. Fabris, G. Fratesi, R. Gebauer, U. Gerstmann, C. Gougoussis, A. Kokalj, M. Lazzeri, L. Martin-Samos, N. Marzari, F. Mauri, R. Mazzarello, S. Paolini, A. Pasquarello, L. Paulatto, C. Sbraccia, S. Scandolo, G. Sclauzero, A. P. Seitsonen, A. Smogunov, P. Umari and R. M. Wentzcovitch, J. Phys.: Condens. Matter, **21**, 395502 (2009).
21. H. J. Monkhorst and J. D. Pack, Phys. Rev. B, **13**, 5188

(1976).
22. C. G. Broyden, J. Inst. Math. Appl., **6**, 76 (1969).
23. A. Dal Corso, J. Phys.: Condens. Matter, **28**, 075401 (2016).
24. V. V. Thanh, D. V. Truong and N. Tuan Hung, Phys. Chem. Chem. Phys., **21**, 22377 (2019).
25. F. Mouhat and F.-X. Coudert, Phys. Rev. B, **90**, 224104 (2014).
26. V. V. Tuan, N. H. Nguyen, A. L. A., Y. K. Q., V. L. Chu, I. K. A., V. P. Huynh and V. H. Nguyen, RSC Adv., **12**, 7973 (2022).
27. V. V. Thanh, N. D. Van, D. V. Truong, R. Saito and N. T. Hung, Appl. Surf. Sci., **526**, 146730 (2020).
28. Q. Peng, W. Ji and S. De, Comput. Mater. Sci., **56**, 11 (2012).

Author Information

Nguyen Hoang Linh
Student, School of Mechanical Engineering, Hanoi University of Science and Technology

Nguyen Minh Son
Student, School of Mechanical Engineering, Hanoi University of Science and Technology

Tran The Quang
Lecturer, Department of Basic Engineering, Faculty of Technology, Thai Binh University

Nguyen Van Hoi
Student, Department of Mechanical System Engineering, Jeonbuk National University

Vuong Thanh
Lecturer, School of Mechanical Engineering, Hanoi University of Science and Technology

Do Van Truong
Associate Professor, School of Mechanical Engineering, Hanoi University of Science and Technology
Associate Professor, International Research Center for Computational Materials Science, Hanoi University